JCB Article

Aberrant myofibril assembly in tropomodulin1 null mice leads to aborted heart development and embryonic lethality

Kimberly L. Fritz-Six,[1] Patrick R. Cox,[2] Robert S. Fischer,[1] Bisong Xu,[2] Carol C. Gregorio,[3] Huda Y. Zoghbi,[2] and Velia M. Fowler[1]

[1]Department of Cell Biology, The Scripps Research Institute, La Jolla, CA 92037
[2]Division of Neuroscience, Department of Pediatrics, and Department of Molecular and Human Genetics, Howard Hughes Medical Institute, Baylor College of Medicine, Houston, TX 77030
[3]Department of Cell Biology and Anatomy, University of Arizona, Tucson, AZ 85724

Tropomodulin1 (Tmod1) caps thin filament pointed ends in striated muscle, where it controls filament lengths by regulating actin dynamics. Here, we investigated myofibril assembly and heart development in a Tmod1 knockout mouse. In the absence of Tmod1, embryonic development appeared normal up to embryonic day (E) 8.5. By E9.5, heart defects were evident, including aborted development of the myocardium and inability to pump, leading to embryonic lethality by E10.5. Confocal microscopy of hearts of E8–8.5 Tmod1 null embryos revealed structures resembling nascent myofibrils with continuous F-actin staining and periodic dots of α-actinin, indicating that I-Z-I complexes assembled in the absence of Tmod1. Myomesin, a thick filament component, was also assembled normally along these structures, indicating that thick filament assembly is independent of Tmod1. However, myofibrils did not become striated, and gaps in F-actin staining (H zones) were never observed. We conclude that Tmod1 is required for regulation of actin filament lengths and myofibril maturation; this is critical for heart morphogenesis during embryonic development.

Introduction

Myofibrils are specialized contractile organelles of striated muscle consisting of functional repeating units, termed sarcomeres. Sarcomere shortening and muscle contraction depends on the assembly and maintenance of a precisely ordered array of antiparallel actin (thin) filaments interdigitating with bipolar myosin (thick) filaments. The uniformity of actin filament lengths in sarcomeres is critical for controlled actin–myosin filament sliding during sarcomere shortening, and determines the length–tension relationship in striated muscles (Littlefield and Fowler, 1998). Many cardiac and skeletal myopathies in humans, as well as in mice and other organisms, result from defects in functions of contractile and sarcomere-associated proteins, while others are likely to result from defects in myofibril assembly and/or turnover (Seidman and Seidman, 2001; Vigoreaux, 2001; Clark et al., 2002). New sarcomere-associated proteins continue to be identified, but their specific contributions to contractile function and/or myofibril assembly are often difficult to dissect, because the molecular mechanisms of de novo myofibril assembly during cardiac and skeletal muscle development in vivo are not well understood (Gregorio and Antin, 2000; Clark et al., 2002).

A key event in myofibril assembly is the regulation of actin polymerization and restriction of actin filament lengths such that all the filaments extend precisely the same distance from the Z disc to the middle of the sarcomere. Light and electron microscopy studies in vertebrates have shown that early in myofibril assembly in vivo, actin filaments are polymerized with α-actinin, titin, and other molecules into precursor Z discs, I-Z-I complexes, in association with the membrane. The I-Z-I complexes then become organized into linear arrays together with bipolar bundles of thick filaments, in which the Z discs are regularly spaced while the actin filaments are overlapping and misaligned with

K.L. Fritz-Six and P.R. Cox contributed equally to this work.

Address correspondence to Velia M. Fowler, Department of Cell Biology, CB163, The Scripps Research Institute, 10550 N. Torrey Pines Road, La Jolla, CA 92037. Tel.: (858) 784-8277. Fax: (858) 784-8753. email: velia@scripps.edu

Key words: actin; tropomodulin; tropomyosin; sarcomere; cardiac muscle

Abbreviation used in this paper: Tmod, tropomodulin.

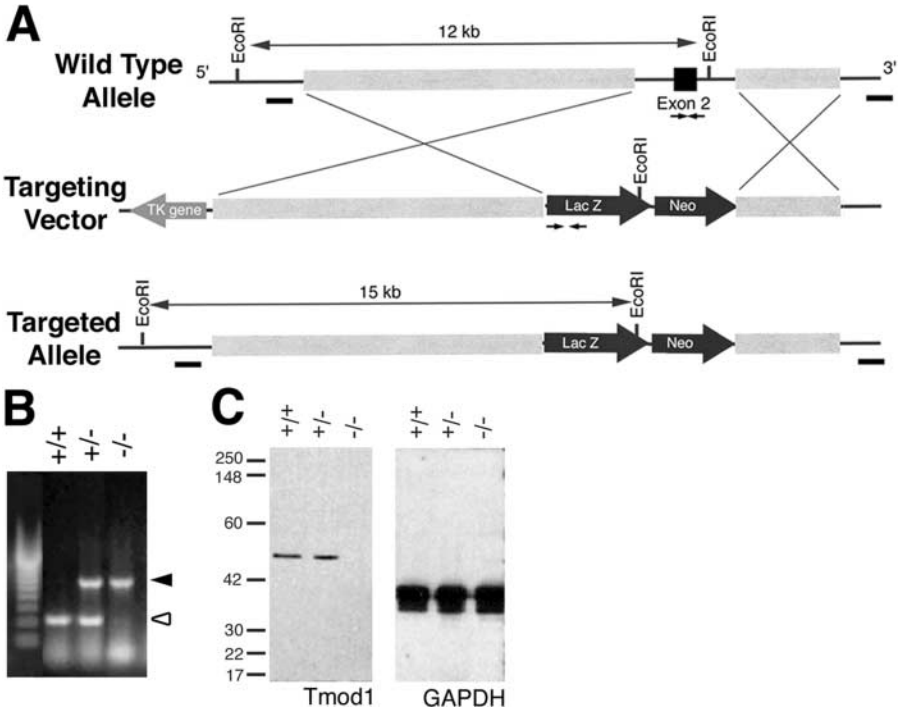

Figure 1. **Targeted disruption of the *Tmod1* gene.** (A) Schematic of expected gene replacement at the *Tmod1* locus. Restriction map of wild-type allele, targeting vector, and targeted allele are shown. *Tmod1* exon 2 is represented as a black box, flanking isogenic genomic DNA as light gray boxes, targeting cassette by thick black arrows, and thymidine kinase gene (selectable marker) by dark gray arrow. Small black bars indicate Southern probes, and sizes of expected fragments after EcoRI digestion are indicated. Small black arrows indicate primers for PCR genotyping. (B) PCR analysis of E10.5 embryonic yolk sac DNA from representative wild-type (+/+), $Tmod1^{lacZ+/-}$ (+/−), and $Tmod1^{lacZ-/-}$ (−/−) embryo. The wild-type allele resulted in a 390-base fragment (open arrowhead), and the recombinant allele in a 1,100-base fragment (closed arrowhead). Left lane is a 200-bp DNA ladder. (C) Western blot of whole E10.5 embryos probed with anti-Tmod1 and GAPDH antibodies. Representative wild type (+/+), $Tmod1^{lacZ+/-}$ (+/−), and $Tmod1^{lacZ-/-}$ (−/−) embryos are shown. Arrowheads, Tmod1 and GAPDH polypeptides.

indeterminate lengths. Subsequently, actin filament lengths are restricted so that their free (pointed) ends all terminate at the edge of the H zone, forming a clear gap in the middle of relaxed sarcomeres (e.g., Markwald, 1973; Tokuyasu and Maher, 1987; Ehler et al., 1999; Rudy et al., 2001; Du et al., 2003; for a recent review see Gregorio and Antin, 2000).

Tropomodulins (Tmods) are a family of conserved actin pointed end capping proteins that regulate actin dynamics and filament length in muscle and nonmuscle cells (Fischer and Fowler, 2003). The predominant isoform in striated muscle is Tmod1 (E-Tmod), which is expressed in embryonic and adult cardiac as well as slow skeletal muscle, where it is associated with the thin filament pointed ends (Fowler, 1996; Almenar-Queralt et al., 1999b). In fast skeletal muscle, the Tmod4 isoform is associated with thin filaments in sarcomeres while Tmod1 is associated with the membrane skeleton at costameres (Almenar-Queralt et al., 1999b). Tmod1 is also present in the membrane skeleton in erythrocytes and lens cells (Fowler, 1996; Fischer and Fowler, 2003). Experiments in living cardiac muscle cells have shown that Tmod1 directly controls thin filament lengths in assembled myofibrils by transiently binding to the thin filament pointed ends and competing for actin monomer addition (Gregorio et al., 1995; Littlefield et al., 2001; for review see Fischer and Fowler, 2003). Regulation of Tmod1 levels is critical for contractile function because cultured cardiac myocytes in which Tmod1 activity or levels have been reduced fail to beat (Gregorio et al., 1995; Sussman et al., 1998a). Tmod1 overexpression in transgenic (TOT) mouse hearts leads to a phenotype reminiscent of dilated cardiomyopathy in humans, including impaired contractility, myofibril degeneration, and alterations in intercalated discs (Sussman et al., 1998b; Ehler et al., 2001). However, a function for Tmod in the restriction of actin filament lengths during de novo myofibril assembly in striated muscle cells has not been established.

To investigate this question, we generated a mouse knockout for the Tmod1 gene, which is expressed in cardiac muscle as well as in erythroid cells in the yolk sac during early embryonic development (Ito et al., 1995). Tmod1 homozygous null animals die during embryogenesis due to defective cardiac development and lack of contractile function. Our results demonstrate that Tmod1 associates with nascent myofibrils before formation of uniform filament lengths, and that the absence of Tmod1 results in the failure of this process, without affecting initial assembly of I-Z-I complexes into nascent myofibrils. Initial assembly of thick filaments, as monitored by myomesin, also appeared to take place in the absence of Tmod1, suggesting that thick filaments can assemble independently of thin filament length regulation. However, in the absence of Tmod1, myofibrils failed to mature and become striated. Subsequent to these defects in myofibril assembly, development of the myocardium was aborted, resulting in inability of the heart to pump. Thus, the absence of Tmod1 leads to a primary defect in de novo myofibril assembly that then results in aborted heart development and embryonic lethality.

Results

Targeted disruption of *Tmod1* leads to lethality of homozygous mutant embryos by E10.5

We produced a targeted deletion of *Tmod1* exon 2 in embryonic stem cells by replacing it with a *β-galactosidase* reporter gene (*lacZ*) (Fig. 1 A). No obvious phenotypes were observed in the adult heterozygous $Tmod1^{lacZ+/-}$ mice as compared with wild-type mice. However, intercrosses of F1

Table I. **Genotypes of offspring from heterozygous matings**

Stage	Total	Genotype		
		+/+	+/−	−/−
E8.5	34	11	17	6
E9.5	18	4	10	4
E10.5[a]	18	4	8	4
E12.5	18	7	11	0
Term	33	13	20	0

[a]Two additional embryos were being resorbed and therefore were unable to be genotyped.

Tmod1$^{lacZ+/-}$ mice did not produce any *Tmod1*$^{lacZ-/-}$ mice in their litters ($n_{offspring}$ = 56, $n_{litters}$ = 9, average litter size = 6.22). To determine the stage of embryonic lethality, timed matings were performed, and embryos were isolated at various stages of gestation. PCR genotyping of yolk sac DNA revealed the presence of *Tmod1*$^{lacZ-/-}$ embryos up until E10.5, but not beyond (Fig. 1 B). The genotypes of embryos examined at E8.5 and E9.5 fit reasonably well to a Mendelian distribution, although by E9–9.5, embryos were visibly abnormal, and by E10.5, embryos were beginning to be resorbed (Table I).

To determine whether the targeted *Tmod1*^{lacZ} allele was a true null, we performed Western blot analysis. While Tmod1 protein was readily detected in wild-type embryos, no Tmod1 protein was present in E9.5–10.5 *Tmod1*$^{lacZ-/-}$ embryos (Fig. 1 C). Interestingly, Tmod1 protein levels in heterozygous *Tmod1*$^{lacZ+/-}$ E9.5 embryos were 1.14 ± 0.24 times the levels in wild-type embryos, which is not significantly different (n = 3, P = 0.24). (Fig. 1 C). Tmod1 protein levels in hearts of adult *Tmod1*$^{lacZ+/-}$ mice were also not significantly different at 1.01 ± 0.13 (n = 3) times the level in wild-type adult hearts. This suggests a dosage-compensation mechanism to restore normal Tmod1 protein levels in the heart, as has been described for α-tropomyosin in the hearts of heterozygous α-tropomyosin knockout mice (Blanchard et al., 1997; Rethinasamy et al., 1998). Myofibril organization was also normal in hearts of adult heterozygous *Tmod1*$^{lacZ+/-}$ mice as assessed by immunofluorescence staining (unpublished data).

Tmod1 is expressed predominantly in the heart from E8–8.5

We determined the expression pattern of the targeted *Tmod1*^{lacZ} allele during embryogenesis by X-gal staining of heterozygous *Tmod1*$^{lacZ+/-}$ embryos staged between E8–8.5 and E13.5. The *Tmod1*$^{lacZ+/-}$ embryos were morphologically indistinguishable from wild-type embryos. X-gal staining was not detected in E8–8.5 embryos but began to be detected after the embryos had turned, at E8.5–9, when it was detected only in the heart (Fig. 2 A). X-gal staining continued to be restricted to the heart in both E9.5 and E10.5 embryos (Fig. 2 A). At E12.5, weak X-gal staining also began to be detected in the otic vesicle and in somites, becoming stronger at E13.5 (Fig. 2 A, right panel, arrow and arrowheads). The lack of *Tmod1*^{lacZ} expression in hearts of E8–8.5 embryos appeared to reflect the insensitivity of the *lacZ* reporter gene expression assay, as Western blot analysis demonstrated that Tmod1 protein was present in these and later stage embryos (Fig. 2 B). Furthermore, immunofluorescence staining demonstrated the presence of Tmod1 in the heart, but not in other tissues, at E8–8.5 (Fig. 2 C); Tmod1 staining in the heart is specific, as no staining was observed in *Tmod1*$^{lacZ-/-}$ embryos (not depicted). We also detected weak staining for Tmod1 in somites of E10.5 embryos as well as low levels of Tmod1 protein on heavily loaded Western blots of yolk sac proteins from E9.5 embryos (not depicted). The expression patterns for the targeted *Tmod1*^{lacZ} allele are consistent with in situ hybridization studies of *Tmod1* mRNA expression that were reported previously by Ito et al. (1995), confirming that the *Tmod1* gene was targeted correctly.

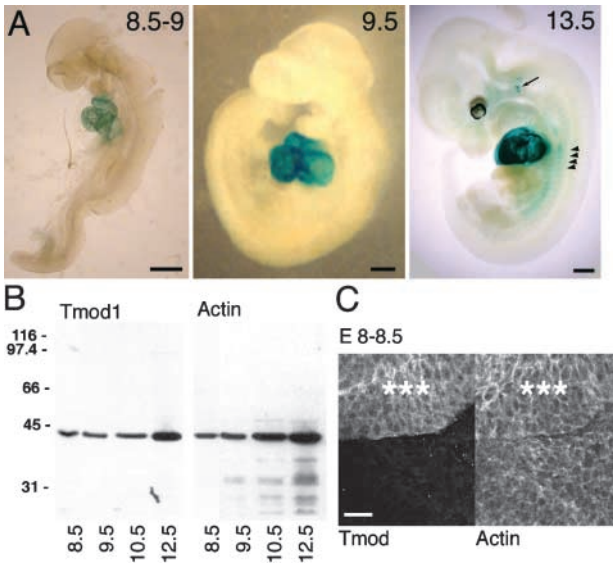

Figure 2. **Tmod1 expression is predominantly in the heart during early embryogenesis.** (A) Whole mount X-gal staining of *Tmod1*$^{lacZ+/-}$ embryos at stages E8.5–9.0, E9.5, and E13.5. Bars: (E8.5–9) 250 μm; (E9.5) 500 μm; (E13.5) 1 mm. *Tmod1*^{lacZ} expression (blue) is observed only in the heart of staged embryos at E8.5–9 and at E9.5. At E13.5, staining is also detected in the otic vesicle (arrow) and in somites (arrowheads). (B) Western blot of wild-type embryos at stages E8–8.5 to E12.5 probed with anti-Tmod1 antibodies, stripped, and then reprobed with a pan actin antibody as a measure of total protein. (C) Low magnification confocal micrographs of wild-type E8–8.5 embryos double stained for Tmod1 (left) and for F-actin with bodipy-phallacidin (right). Tmod1 protein staining is only in heart cells, identified by double staining with sarcomeric α-actinin (see Fig. 3). Location of heart cells is indicated by asterisks. Bar, 50 μm.

Tmod1 null embryos are grossly stunted and malformed with aborted development of the myocardium at mid-gestation

Observation of the gross morphology of *Tmod1*$^{lacZ-/-}$ embryos revealed that at E8–8.5 before the embryos had turned, the mutant embryos were comparable to wild-type embryos in size and morphology, appearing remarkably normal (Fig. 3, A and B). Similarly, histological analysis of *Tmod1*$^{lacZ-/-}$ embryos revealed that it was difficult to distinguish the wild-type and null hearts at E8–8.5 (Fig. 3, C–F). However, by E9.5, the *Tmod1*$^{lacZ-/-}$ embryos were considerably smaller than their wild-type littermates and

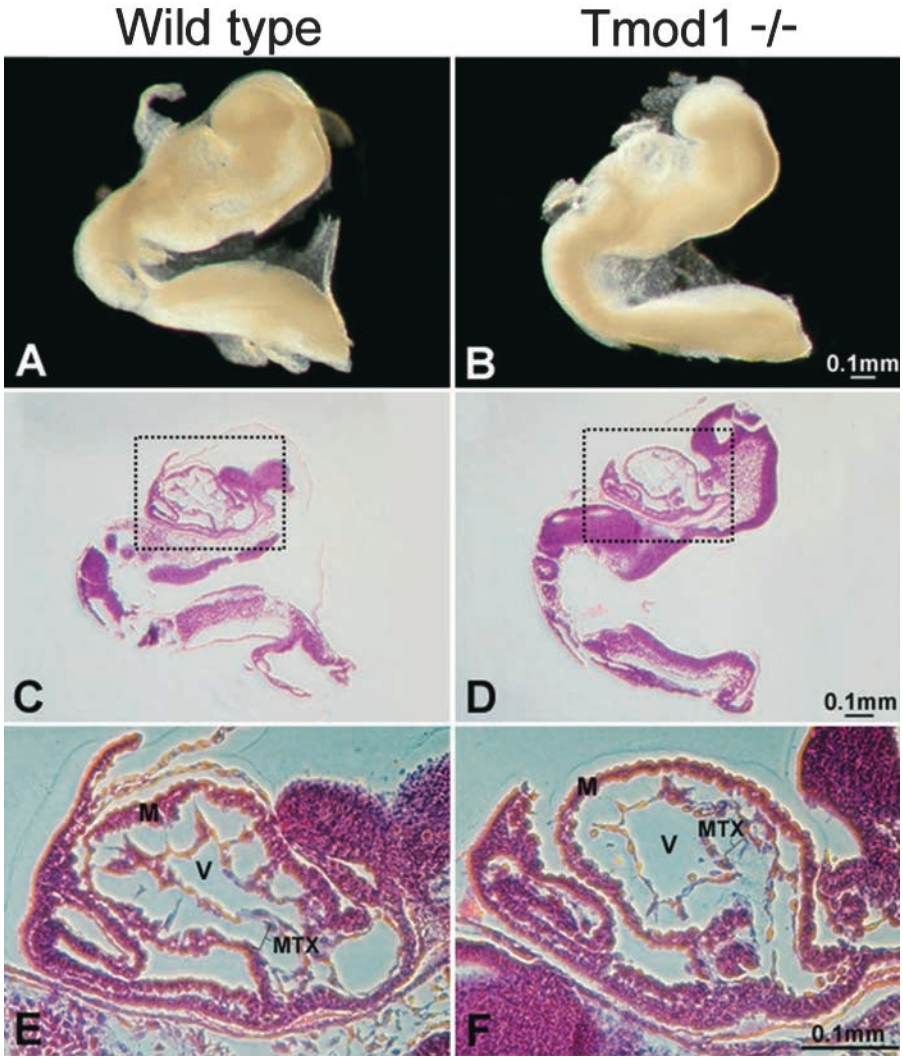

Figure 3. **Tmod1$^{lacZ-/-}$ embryos appear normal at E8–8.5.** Whole mounts and histological analysis of E8–8.5 wild-type (A, C, and E) and Tmod1 null (B, D, and F) embryos. Sagittal sections of wild-type (C and E) and null (D and F) embryos are shown. Note the seemingly normal overall morphological appearance of the knockout embryo at E8–8.5, as well as the normal early myocardium and matrix in the mutant heart tube (low and high magnification view in D and F, respectively), in comparison to wild type (low and high magnification view in C and E, respectively). V, ventricle; M, myocardium; MTX, matrix.

exhibited obvious defects in development of the head structures (Fig. 4, A and B). At this stage, although there was variability in the severity of the phenotype, all the hearts from *Tmod1*$^{lacZ-/-}$ embryos demonstrated aborted myocardial development (Fig. 4, D and F). While no loss of extracellular matrix in the ventricle was detected, the myocardium was abnormally thin in the mutant *Tmod1*$^{lacZ-/-}$ embryos (approximately two cell layers thick) and appeared to lack well-defined trabeculations (Fig. 4 F) in comparison to the wild-type embryos (Fig. 4 E). Although not evident in the image of this particular section, pooling of erythrocytes in the malformed heart cavity of the mutant E9.5 embyros was observed frequently (not depicted), suggestive of defective contractile function (Fig. 5). The gross morphology of the embryonic yolk sac was normal at E8.5, but by E9–9.5, it had become very wrinkled and folded (unpublished data). Embryos from *Tmod1*$^{lacZ-/-}$ mice failed to grow any further, and by E10.5, embryos were very small and misshapen with a distended pericardial cavity containing the malformed heart (not depicted). The distension of the pericardial cavity likely resulted from fluid leakage into the pericardium, and has been observed in a separate study of another Tmod1 knockout mouse (Chu et al., 2003) as well as in other knockout mice with aborted cardiac development (e.g., Radice et al., 1997).

The hearts of Tmod1 null embryos do not beat

To determine the effect of Tmod1 deficiency on embryonic heart function, we isolated *Tmod1*$^{lacZ-/-}$ and wild-type E9.5 living embryos and cultured them at 37°C for several hours (Luo et al., 2001). The hearts of wild-type embryos beat steadily and strongly (every 2–3 min) for >6 h under these conditions. In contrast, the hearts of the *Tmod1*$^{lacZ-/-}$ embryos did not beat at all and only twitched once or twice during the first 15–20 min after isolation and in response to initial contact with the microinjection needle. India ink injected into the heart chamber of wild-type E9.5 embryos was distributed (pumped) throughout the vasculature (Fig. 5 A). In contrast, ink injected into the heart chamber of *Tmod1*$^{lacZ-/-}$ E9.5 embryos remained in close proximity to the misshapen heart and gradually leaked out passively (Fig. 5 B) ($n = 3$). In some mutant embryos, the ink appeared to enter the proximal portions of vessels as a result of the pressure produced during the microinjection procedure, but never progressed any further. Thus, the hearts of embryos that are lacking Tmod1 do not have functional contractile activity.

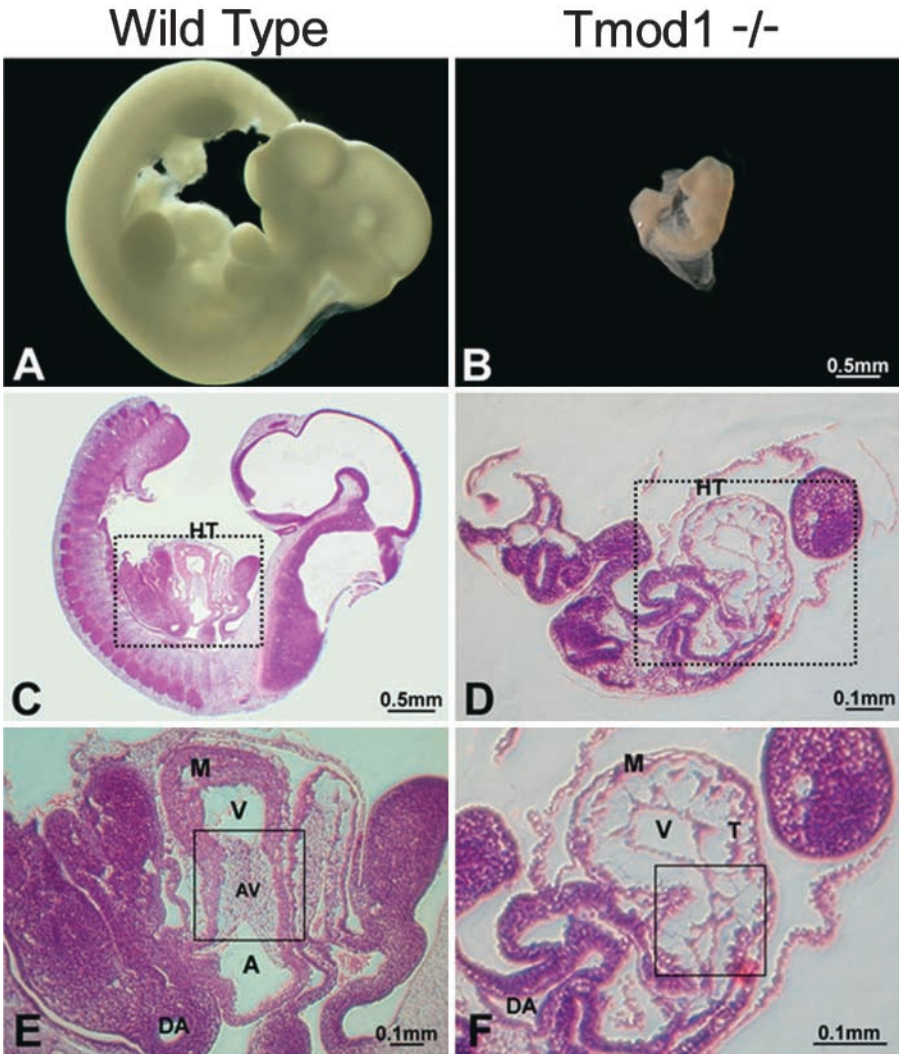

Figure 4. **Tmod1$^{lacZ-/-}$ embryos display aberrant embryonic and cardiac development at E9.5–10.** Whole mounts and histological analysis of E10 wild-type (A, C, and E) and E9.5 Tmod1 null (B, D, and F) embryos. Sagittal sections of wild-type (C and E) and null (D and F) embryos are shown. Severely underdeveloped myocardium and trabeculation (T) of the left ventricle are apparent in the null embryos (low and high magnification view in D and F, respectively) in comparison to wild type (low and high magnification view in C and E, respectively). Note, in boxed in regions, complete lack of cellularization within the AV canal in mutant (F), in comparison to wild type (E). V, ventricle; A, atrium; M, myocardium; DA, dorsal aorta; T, trabeculations; AV, AV canal; HT, heart.

Tmod1 assembles into nascent myofibrils at E8–8.5 of embryonic development

To investigate the consequences of Tmod1 deletion on myofibril assembly and actin filament length regulation, we first determined the assembly properties of Tmod1 during de novo myofibril assembly in the murine heart. We performed confocal immunofluorescence microscopy using antibodies to Tmod1 and sarcomeric α-actinin, a well-characterized marker for myofibril assembly (e.g., Holtzer et al., 1997; Ehler et al., 1999; Du et al., 2003) (Fig. 6). In cardiac myocytes of E8–8.5 embryos, Tmod1 staining was frequently concentrated between periodic dots of sarcomeric α-actinin, suggesting Tmod1 association with thin filament pointed ends between I-Z-I complexes in nascent myofibrils (Fig. 6, top). Tmod1 was also present in a diffuse pattern in the cytoplasm in the hearts of E8–8.5 embryos, likely due to a pool of unassembled Tmod1 (Gregorio and Fowler, 1995), making it difficult to detect Tmod1 on many of the sarcomeric α-actinin–containing nascent myofibrils (Fig. 7). Later, in hearts from E9.5 embryos, the diffuse staining for Tmod1 in the cytoplasm decreased, and the Tmod1 striations became more defined in the center of sarcomeres of many myofibrils, alternating with α-actinin striations (Fig. 6, middle). By E12.5, both Tmod1 and α-actinin striations were organized in a relatively mature pattern (Fig. 6, bottom). Note that the sarcomeres in these embryos were somewhat contracted, thus leading to the presence of a single Tmod1 band rather than a

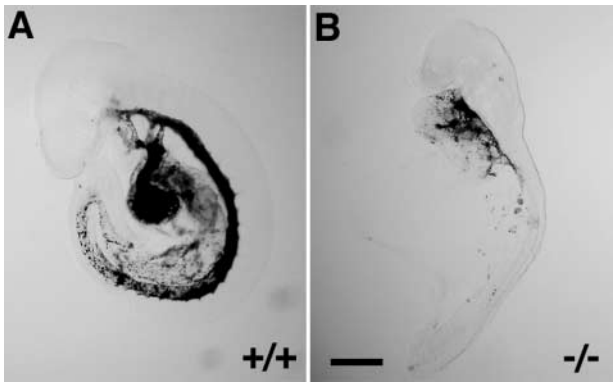

Figure 5. **The hearts of Tmod1 null embryos fail to pump.** Living E9.5 embryos were microinjected with India ink into the right ventricle, and the heart was allowed to pump the ink through the vasculature. (A) Ink injected into wild-type embryos (+/+) was pumped throughout the vasculature, while (B) ink injected into the *Tmod1*$^{lacZ-/-}$ embryos (−/−) stayed within the heart tube, dispersing by passive diffusion over 6 h in culture. Bar, 1 mm.

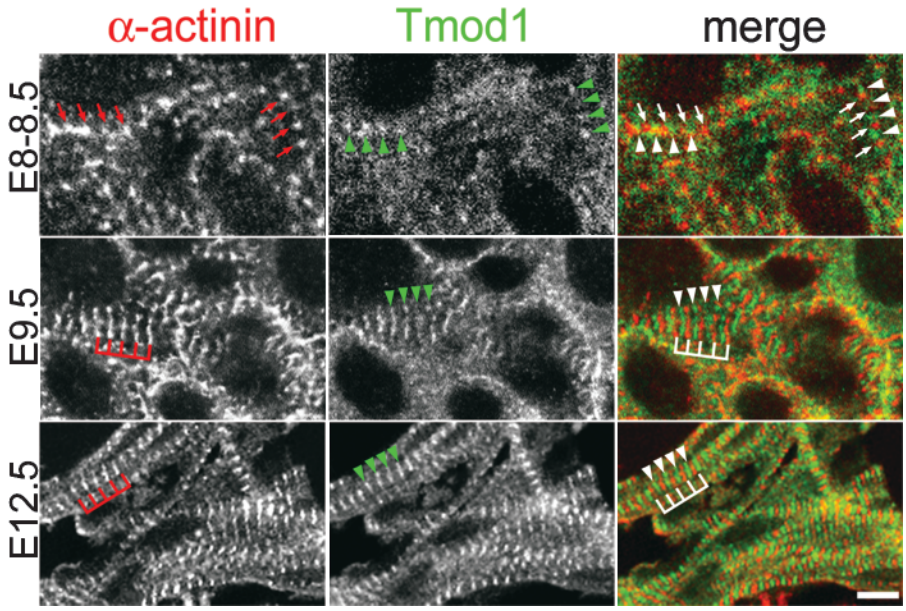

Figure 6. **Tmod1 and sarcomeric α-actinin assembly into myofibrils in the heart during early embryogenesis of wild-type embryos.** Confocal fluorescence micrographs of hearts of staged wild-type embryos at E8–8.5, E9.5, or E12.5 double stained with a rabbit antibody to Tmod1 and a mouse monoclonal antibody to sarcomeric α-actinin. Merge: Tmod1, green; α-actinin, red. Arrows, periodic α-actinin dots; brackets, α-actinin striations; arrowheads, Tmod1. Bar, 10 μm.

doublet in the center of sarcomeres (Gregorio and Fowler, 1995; Littlefield et al., 2001).

We next investigated the timing of Tmod1 assembly into myofibrils with respect to the appearance of gaps in F-actin staining in the middle of the sarcomeres, indicative of regulated actin filament lengths. For these experiments, E8–8.5 embryos were pretreated with a relaxing buffer before fixation so that sarcomeres would be long enough to reveal gaps in F-actin staining in the middle of the sarcomere (Granzier et al., 1996). Triton X-100 was also included to reduce the levels of cytoplasmic staining for Tmod1. In E8–8.5 embryos (Fig. 7, top and middle), Tmod1 was associated with many types of F-actin–containing fibrillar structures, including those that stained fairly evenly along their length, those with brighter and dimmer regions of F-actin staining, and others with gaps in F-actin staining resembling mature myofibrils (middle row, inset). Strikingly, the Tmod1 staining was frequently discontinuous and was concentrated in broad bands that often coincided with decreases or discontinuities in F-actin staining (Fig. 7, arrowheads). These concentrations of Tmod1 may indicate the location of actin filament pointed ends, reflecting the presence of actin filaments whose lengths are not yet precisely regulated in the nascent myofibrils. Even in sarcomeres with clear gaps in F-actin staining, the Tmod1-stained bands were often broad and poorly defined (Fig. 7, inset), suggesting that there were many actin filaments with variable lengths in myofibrils of E8–8.5 embryos. Later, in E9.5 embryos, the Tmod1 striations were sharper and better defined (Fig. 7, bottom), similar to Tmod1 in mature myofibrils (Gregorio and Fowler, 1995; Littlefield et al., 2001). Significantly, in contrast to our previous studies on myofibril assembly in cultured chick cardiac myocytes and precardiac explants (Gregorio and Fowler, 1995; Rudy et al., 2001), no myofibrils with gaps in

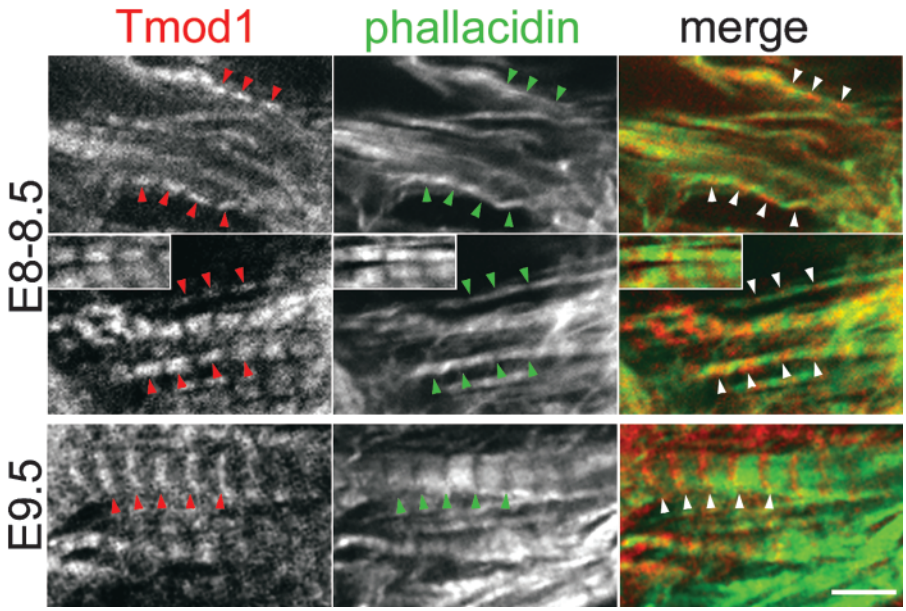

Figure 7. **Tmod1 and F-actin assembly into myofibrils in the heart of E8–8.5 and E9.5 wild-type embryos.** Confocal fluorescence micrographs of relaxed embryonic hearts at stage E8–8.5 (first and second rows) or E9.5 (third row), double stained with a rabbit antibody to Tmod1 and bodipy-phallacidin for F-actin. Merge: F-actin, green; Tmod1, red. Arrowheads, Tmod1 concentrations at decreases or discontinuities in F-actin staining (E8–8.5) and at gaps in F-actin in E9.5 embryos. Inset, Tmod1 concentrations at gaps in F-actin staining in a myofibril from a different region of the same image of an E8–8.5 embryo. Note that the inset is at the same magnification as other panels. Bar, 5 μm.

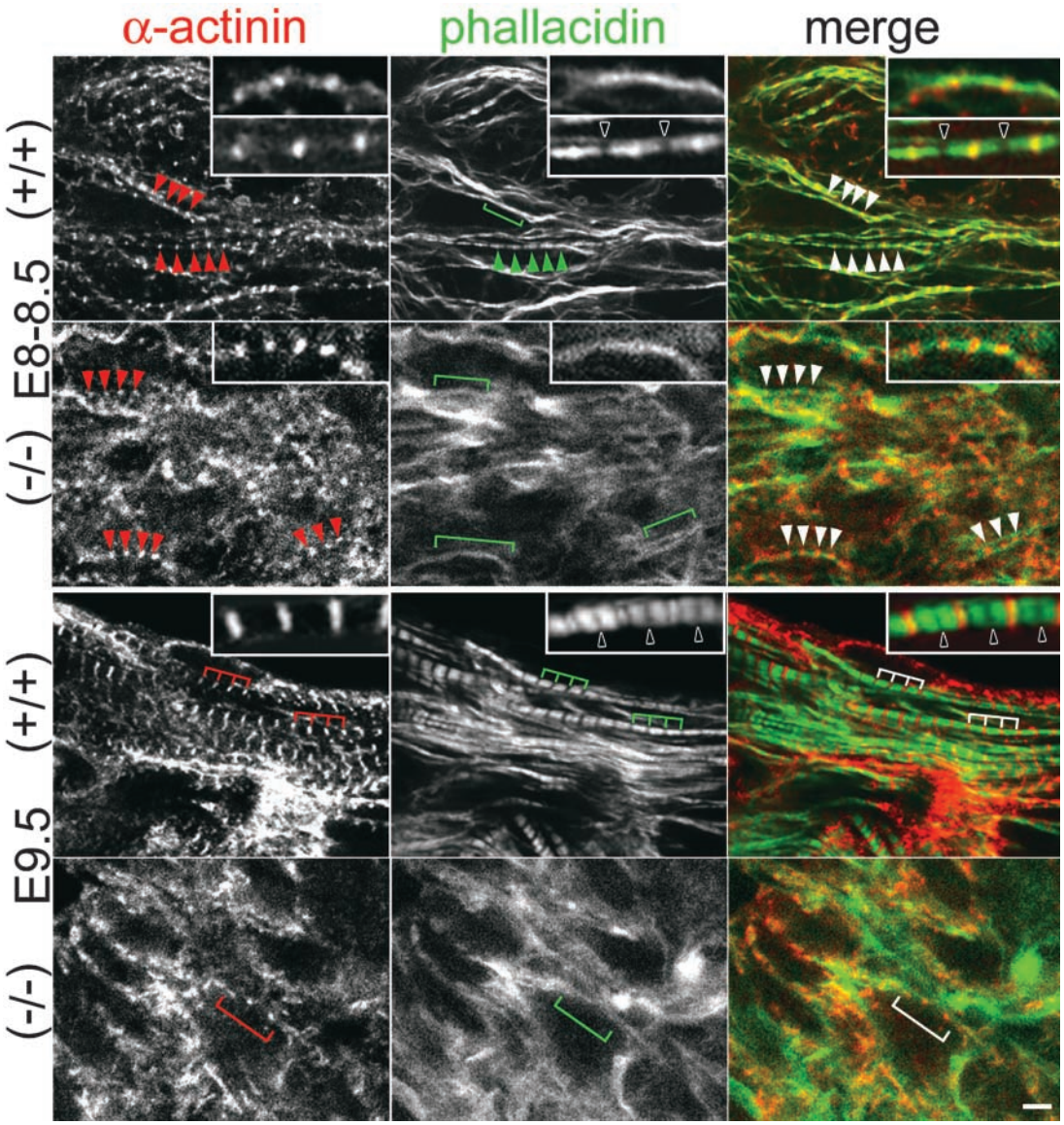

Figure 8. **Myofibrils do not become striated in hearts of *Tmod1*$^{lacZ-/-}$ embryos.** Confocal fluorescence micrographs of hearts of wild-type (+/+) and *Tmod1*$^{lacZ-/-}$ (−/−) embryos from stages E8–8.5 and E9.5, double stained with a monoclonal antibody to sarcomeric α-actinin and bodipy-phallacidin for F-actin. Merges: α-actinin, red; bodipy-phallacidin, green. Arrowheads, α-actinin dots along nascent myofibrils. Short brackets, α-actinin striations at Z discs. Long brackets, regions of continuous F-actin staining. Bar, 5 μm. Insets: 2× higher magnification images of representative nascent and mature myofibrils from the stages indicated. Open arrowheads in insets, gaps in F-actin staining.

F-actin staining were observed that did not also contain Tmod1. Thus, in the mouse heart, our observations suggest that Tmod1 is associated with thin filament pointed ends in assembling myofibrils both before and during the formation of regulated filament lengths.

Myofibril assembly is aberrant in hearts of Tmod1 null embryos

To investigate the basis for aborted cardiac development and the lack of contractile function in Tmod1 null embryos, we compared myofibril assembly and organization in hearts of embryos from wild-type and Tmod1 null mice. We first analyzed sarcomeric α-actinin and F-actin organization in E8–8.5 embryos, a stage when mutant embryos were normal by gross morphology and by histological analysis (Fig. 3). At this stage of development in wild-type embryos (Fig. 8, top row), myofibrils at varying stages of maturity were observed, including nascent myofibrils with irregular and/or periodic dots of sarcomeric α-actinin (arrowheads) and continuous F-actin staining (long brackets and top inset). Apparently mature, but very thin, myofibrils were also present at this stage, with regularly spaced dots of sarcomeric α-actinin (arrowheads) alternating with distinct and periodic gaps in F-actin staining (inset, open arrowheads). In Tmod1 null embryos from the same stage of development (Fig. 8, second row), periodic dots of sarcomeric α-actinin (arrowheads) were frequently observed along structures with continuous F-actin staining (long brackets and inset), but distinct gaps in F-actin staining were never observed. Additionally, aggregates of sarcomeric α-actinin and F-actin that did not colo-

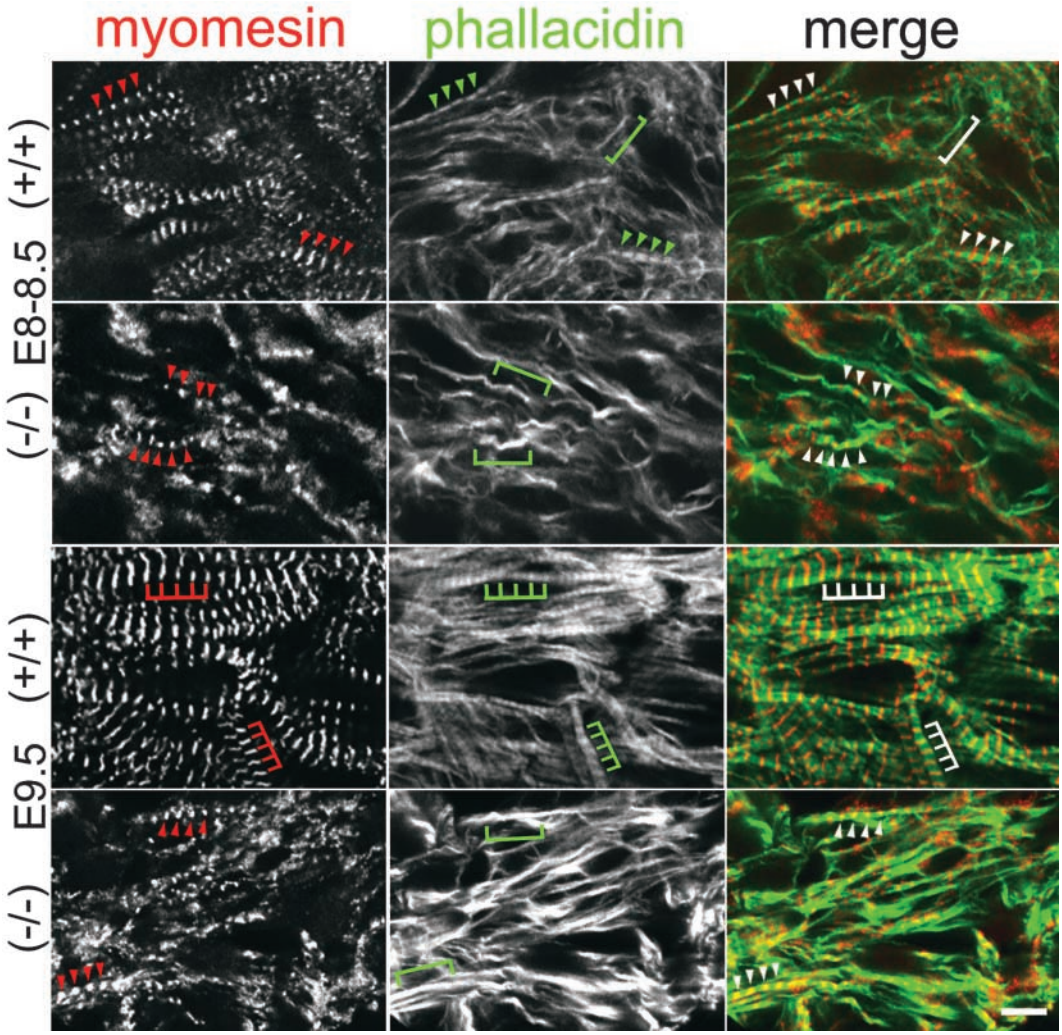

Figure 9. **Myomesin assembles into myofibrils in *Tmod1*$^{lacZ-/-}$ embryos.** Confocal fluorescence micrographs of hearts of wild-type (+/+) and *Tmod1*$^{lacZ-/-}$ (−/−) embryos from stages E8–8.5 and E9.5, double stained with a monoclonal antibody to myomesin and bodipy-phallacidin for F-actin. Merges: myomesin, red; bodipy-phallacidin, green. Arrowheads, periodic myomesin dots along assembling myofibrils. Short brackets, mature myomesin striations. Long brackets, regions of continuous F-actin staining. Bar, 5 μm.

calize with one another were present in some regions of the cells from the mutant embryos at this stage.

We next compared sarcomeric α-actinin and F-actin organization in wild-type and Tmod1 null embryos at E9.5, a stage when Tmod1 was present in distinct, narrow striations at thin filament pointed ends in wild-type embryos (Figs. 6 and 7), and when histological abnormalities in the heart were now observed in mutant embryos (Fig. 4). At this stage of development in wild-type embryos, myofibrils exhibited regular sarcomeric α-actinin striations characteristic of mature Z discs, along with a striated F-actin staining pattern with gaps (Fig. 8, third row, inset). In contrast, in the Tmod1 null E9.5 embryos, no striated myofibrils could be found, and nascent myofibril-like structures with dots of sarcomeric α-actinin were rarely observed (Fig. 8, bottom, long bracket). Instead, most sarcomeric α-actinin and F-actin appeared to be disorganized and to have accumulated into large aggregates. This suggests that the nascent myofibril-like structures in the E8–8.5 mutant embryos may have disassembled and/or aggregated by E9.5.

In summary, the most striking observation from this analysis is that nascent myofibrils had assembled in the absence of Tmod1, but never matured into striated myofibrils with gaps at the H zone. This demonstrates that Tmod1 function is required for the relatively late event of restriction of actin filament lengths but not for initial assembly of I-Z-I complexes into nascent myofibrils. Furthermore, defects in myofibril assembly in the absence of Tmod1 appear to be upstream of defects in cardiac development or in other embryonic structures, as myofibril assembly was already disrupted in E8–8.5 mutant embryos, a stage when no gross morphological or histological changes were observed (Fig. 3).

Assembly of the thick filament–associated protein, myomesin, does not require Tmod1

Previous studies on myofibril assembly have indicated that thick filament assembly may be independent of thin filament assembly (Markwald, 1973; Epstein and Fischman, 1991; Holtzer et al., 1997). Therefore, we investigated the assembly of myomesin, an M-line protein that is associated

with thick filaments (Auerbach et al., 1997; Ehler et al., 1999). In E8–8.5 wild-type embryos, myomesin was observed in a periodic dot-like or striped pattern along the myofibrils (depending on their thickness), where it colocalized with gaps in F-actin staining (Fig. 9, top). Unlike sarcomeric α-actinin (Fig. 8, top), myomesin was not associated with structures that stained continuously for F-actin (Fig. 9, top, long bracket). This is similar to studies in other systems showing that myomesin and thick filaments assemble into myofibrils subsequent to sarcomeric α-actinin and I-Z-I complexes (Auerbach et al., 1997; Ehler et al., 1999). Later in development, in E9.5 wild-type embryos, striations of myomesin became increasingly obvious, due to lateral alignment of the myofibrils (Fig. 9, third row, short brackets). Note that the myofibrils in this particular E9.5 wild-type embryo were contracted, resulting in brighter F-actin staining in the middle of the sarcomere where the thin filament pointed ends overlapped (for a discussion of phalloidin staining see Littlefield and Fowler, 2002).

In E8–8.5 and E9.5 Tmod1 null embryos, short sets of periodic myomesin dots (arrowheads) were frequently found located along structures with continuous F-actin staining (long brackets) (Fig. 9), similar to sarcomeric α-actinin (Fig. 8). However, myomesin staining never became striated, even in E9.5 mutant embryos, and gaps in F-actin staining were never observed along the myomesin-stained structures (Fig. 9, long brackets). Independent aggregates of myomesin and F-actin that did not colocalize with one another were also a predominant feature in the cells from the mutant embryos at both E8.5 and E9.5 (Fig. 9), as shown above for sarcomeric α-actinin (Fig. 8). The presence of aggregates of myomesin could be due to disassembly of the nascent myofibril-like structures in the absence of Tmod1 followed by aggregation, and/or to direct accumulation of myomesin into ectopic aggregates by an aberrant assembly pathway.

In conclusion, similar to sarcomeric α-actinin, the initial assembly of myomesin into nascent myofibrils does not appear to require the presence of Tmod1 and does not require that actin filament lengths be regulated. As myomesin is an integral thick filament component, this result also suggests that thick filaments can assemble into nascent myofibrils in the absence of Tmod1.

Discussion

Here, we show that the absence of Tmod1 in the heart results in failure of myofibril assembly, aborted cardiac development, and embryonic lethality at mid-gestation. Nascent myofibril-like structures with overlapping actin filaments and regularly spaced dots of sarcomeric α-actinin formed in the absence of Tmod1, but failed to progress to striated myofibrils with regulated actin filament lengths. Myomesin, an integral thick filament component at the M-line, was also found assembled in a periodic fashion along nascent myofibril-like structures in the absence of Tmod1. Thus, the initial assembly of both Z disc (α-actinin) and thick filament components (myomesin) were independent of actin filament length regulation by Tmod1. However, in the absence of Tmod1, nascent myofibrils appeared unstable, leading to aberrant aggregation of individual thin and thick filament components, as described here by immunofluorescence microscopy and in an independent study by electron microscopy (Chu et al., 2003). This indicates that Tmod1 is an essential structural component of sarcomeres. It is required for formation of regulated actin filament lengths, as well as for myofibril maturation and sarcomeric integrity during de novo myofibril assembly in the developing heart.

The aborted cardiac development observed in the homozygous null Tmod1 embryos is likely a direct consequence of the absence of Tmod1 in the cardiac myocytes. Tmod1 mRNA (Ito et al., 1995) and protein (this study) are first detected only in the wild-type embryonic heart at E8–8.5, when defects in myofibril assembly are observed in Tmod1 null embryos. Significantly, aberrant myofibril assembly was already detected at E8–8.5, before any abnormalities in embryonic or cardiac development were evident by histological analysis. Failure to assemble myofibrils resulted in aborted development of the myocardium so that the extent of heart development of E9.5 mutant embryos resembled that of E8–8.5 embryos. The mechanism by which aberrant myofibril assembly leads to aborted development of the myocardium is not clear, and may involve indirect signaling mechanisms (Ehler et al., 2001; Clark et al., 2002). However, defective cardiac development is unlikely to be due to inadvertent targeting of another gene because a similar phenotype was observed in a Tmod1 knockout mouse created by targeted deletion of exon 1 of the Tmod1 gene (Chu et al., 2003), rather than deletion of exon 2 (this study). Furthermore, analysis of the expression patterns of myosin light chains 2a and 2v and the transcription factors eHAND and dHAND in the hearts of these Tmod1 null mice also showed that developmental specification of atrioventricular chambers appeared to take place by E9.0, although the right ventricle was underdeveloped (Chu et al., 2003).

Given the complete lack of normal myofibrils and aberrant development of the myocardium, it is not surprising that the hearts of these Tmod1 mutant embryos were incapable of contractile function (this study; Chu et al., 2003). The inability of the heart to pump can explain pooling of red blood cells in the abnormal heart cavity of the mutant embryos, defects in vascular development in the yolk sac, the severe retardation of embryonic growth, and subsequent embryonic lethality at E10.5 (this study; Chu et al., 2003). Retardation in embryonic growth may also be due partly to hemolytic anemia resulting from abnormal erythrocyte function in Tmod1 null embryos. Tmod1 mRNA is expressed in primitive erythroid cells in the developing blood islands at E8–8.5 (Ito et al., 1995; Chu et al., 2003), and Tmod1 protein is detected in yolk sacs by Western blot analysis at this stage (this study). In fact, analysis of the mechanical properties of primitive erythroid cells from Tmod1 null embryos demonstrates that the cells are abnormally fragile and subject to mechanical hemolysis (Chu et al., 2003).

How might Tmod1 participate in the regulation of actin filament lengths during the transition of nascent to mature myofibrils in wild-type embryos? Any mechanism must take into account our observation that Tmod1 is associated with nascent myofibrils at early stages during de novo myofibril assembly in the developing murine heart. Strikingly, Tmod1

appeared to localize in an increasingly regular, striated pattern along the nascent myofibrils coincident with the appearance of discontinuities or gaps in F-actin staining, similar to our previous observations of de novo myofibril assembly in cultured chick skeletal myotubes (Almenar-Queralt et al., 1999a). In other words, Tmod1 is associated with myofibrils early, but becomes organized in a striated pattern late, due to alignment of thin filament pointed ends at the edges of the forming H zones. Although we had proposed earlier that nascent myofibrils could become striated due to rearrangements of Tmod1-capped actin filaments without changes in their length (Almenar-Queralt et al., 1999a), this mechanism assumed that Tmod1 capping of filament ends was irreversible, which is not the case (Littlefield et al., 2001). In fact, Tmod1 capping of actin pointed ends is dynamic, allowing continuous exchange of actin monomers at filament ends, and Tmod1 alters filament length via its dynamic capping ability. Thus, we propose that variable length actin filaments in nascent myofibrils are actively shortened (or elongated) by actin monomer dissociation and association as Tmod1 comes on and off the filament ends. In this case, actin filament lengths would tend to equilibrate eventually at lengths where Tmod1 capping affinity is the strongest (for a discussion see Fischer and Fowler, 2003). If Tmod1 capping affinity were regulated by a template or ruler protein such as titin or nebulin, then filament lengths would tend toward this length. Such a mechanism has been proposed for skeletal muscle, based on binding of Tmod1 to the extreme NH_2-terminal end of nebulin (Littlefield and Fowler, 1998; McElhinney et al., 2001), and more recently for cardiac muscle (Kazmierski et al., 2003).

An unexpected finding from our analysis of myofibril assembly was that thin filaments and myofibrils appeared to be unstable in the absence of Tmod1, forming aberrant aggregates rather than progressing to striated myofibrils. Thus, in addition to length regulation, Tmod1 may function to reduce actin filament turnover at the pointed end, stabilizing the thin filaments in myofibrils. How could this work? First, Tmod1 binding to actin at pointed ends may directly antagonize the ability of cofilin/ADF proteins to induce dissociation of actin monomers from filament pointed ends (Bamburg et al., 1999; Fischer and Fowler, 2003). Second, Tmod1 binds to tropomyosin at pointed ends and enhances the ability of tropomyosin to prevent actin pointed end depolymerization (Weber et al., 1994, 1999). Third, stabilization of tropomyosin–actin interactions by Tmod1 could additionally promote the ability of tropomyosin to block filament severing and depolymerization by cofilin/ADF proteins or by gelsolin (Nyakern-Meazza et al., 2002; Ono and Ono, 2002, and references therein). In fact, Tmod1 binding to tropomyosin at actin filament pointed ends has been shown to enhance thin filament stability in cultured chick cardiac myocytes (Mudry et al., 2003). Disruption of Tmod1–tropomyosin interactions in these cells resulted in dissociation of Tmod1, followed by tropomyosin disassembly and actin filament depolymerization from the thin filament pointed ends. Therefore, we propose that in the mouse heart, increased thin filament instability and turnover in the absence of Tmod1 could result in myofibril disassembly followed by accumulation of components in aberrant aggregates, as we observe (also see Chu et al., 2003).

Additional support for the idea that myofibril assembly and stability depends on coordinate regulation of actin filament polymerization and depolymerization comes from genetic analysis of myofibril assembly in the Unc-60B mutant in *Caenorhabditis elegans* (Ono et al., 1999; Ono and Ono, 2002). Unc-60B is the nematode homologue of cofilin/ADF. In the absence of Unc-60B, normal myofibrils do not assemble, and large aberrant actin filament bundles accumulate in the cytoplasm. Significantly, feeding wild-type worms siRNA to reduce tropomyosin levels also results in similar aberrations in myofibril assembly (Ono and Ono, 2002). The deleterious effects of tropomyosin reduction are reversed in an Unc-60B mutant background, indicating that tropomyosin normally protects the actin filaments in assembling myofibrils against the filament severing and disassembly activity of Unc-60B. These experiments, together with our results, suggest that actin filament assembly in myofibrils may depend on a balance between actin stabilization by Tmod with tropomyosin, and actin disassembly mediated by cofilin/ADF (Fischer and Fowler, 2003).

Genetic analyses of myofibril assembly and muscle function in mice, zebrafish, flies, and worms reveal that Tmod1 fits into the category of sarcomere components that are essential for de novo myofibril assembly. These include actin and myosin, the myofibril template protein, titin, and the thin filament components, tropomyosin and troponin T (for reviews see Epstein and Fischman, 1991; Littlefield and Fowler, 1998; Gregorio and Antin, 2000; Vigoreaux, 2001; Sehnert and Stainier, 2002, and references therein). However, Tmod1 is the first sarcomeric component shown to be essential for a specific, discrete step of de novo myofibril assembly in the developing murine heart; namely, restriction of actin filament lengths at the H zone. Furthermore, while formation of M-lines and H zones are both relatively late events in myofibril assembly, our results show that they likely proceed by independent, parallel pathways. It can be anticipated that analysis of myofibril assembly during cardiac development in other mutant embryos by immunofluorescence staining with probes for specific sarcomeric components will further define pathways for myofibril assembly in vivo.

Materials and methods

Generation of *Tmod1*$^{lacZ-/-}$ mice

The genomic structure of the mouse Tmod1 gene is published (Chu et al., 2000). A rat Tmod1 cDNA (Watakabe et al., 1996) was used to screen a mouse 129/SvEv genomic library. 18 clones were identified, of which #10C was the most 5′ and contained coding exon 2. This clone was characterized by restriction mapping and sequencing and used to produce a homologous recombination construct, Tmod1^{lacZ}. 10- and 2.5-kb isogenic genomic DNA fragments flanking exon 2 acted as the 5′ and 3′ homologous arms around a lacZ-neo cassette (Friedrich and Soriano, 1991). The neomycin resistance gene provided positive selection; negative selection was produced by a thymidine kinase cassette outside the 3′ arm. 25 μg of the construct was linearized by Kpn I digestion and electroporated into AB2.1 129 Sv/Ev ES cells using a GenePulser (Bio-Rad Laboratories) set at 300 V and 500 μF. 300 colonies were picked after selection with G418 and gancyclovir, and transferred in triplicate into 96-well plates. DNA from ES cell colonies was analyzed (Ben-Arie et al., 1997), digested with BamHI, and analyzed by Southern hybridization using either a 5′ or 3′ genomic probe outside of the homologous arms of the targeting construct. Positive ES cell clones F11, C11, and B9 were expanded and injected into the inner cell mass of C57BL/6J blastocysts. The resulting male chimeras were bred to C57BL/6J female mice, but only ES cell line C11 achieved

germline transmission. Due to a BamHI restriction fragment length polymorphism between 129/SvEv and C57BL/6J, progeny were genotyped using EcoRI digestion, which produced a 12-kb endogenous or a 15-kb recombinant DNA fragment. F1 mice were backcrossed for one generation on to a C57BL/6J background, and subsequent analysis was performed on intercrosses of these mice. Genomic DNA was isolated from mouse tails or yolk sacs, and mice or staged embryos were genotyped by PCR using one set of primers corresponding to the lacZ gene and the other corresponding to exon 2 of the Tmod1 gene.

Western blotting

SDS lysates were prepared by homogenization and sonication in 20 volumes of SDS sample buffer, followed by boiling 5 min and centrifugation in an Eppendorf microfuge to clarify. SDS-gel samples were electrophoresed on 12% minigels and transferred to nitrocellulose for Western blotting with affinity-purified rabbit antibodies to human Tmod1 (R1749) (Fowler et al., 1993) and chemiluminescence detection. These antibodies were specific for the Tmod1 isoform in mice (not depicted). In some experiments, blots were probed with a monoclonal antibody to striated muscle α-actin (HUC-1) or a pan-actin antibody (C4) (gifts from J. Lessard, University of Cincinnati, Cincinnati, OH). Tmod1 levels were quantified using [^{125}I]protein A (Fowler et al., 1993). To control for loading, blots were stripped and reprobed with an antibody to GAPDH (Biogenesis). Within the gel buffer system used, prestained marker proteins run faster than unlabeled proteins, giving a larger apparent size for Tmod1 (Fig. 1 C and Fig. 2 B).

Morphological and histological analysis

Timed pregnant mice were killed at various days post coitum, and embryos were dissected free of the decidua in PBS and fixed overnight in Bouin's solution. Embryos were washed in 70% ethanol and dehydrated in an ethanol series for paraffin embedding, sectioning, and staining with hematoxylin and eosin. Multiple serial sections were stained and analyzed for each time point and genotype. Whole mount X-gal staining was by the method of Bonnerot and Nicolas (1993). Staining was at 30°C for 24 h, and embryos were washed in fresh PBS followed by fixation overnight in buffered formalin at 4°C. Older embryos (E10–13.5) were dehydrated in ethanol and cleared in 100% methyl salicylate. Embryos were staged by the day post coitum, gross morphology, and somite number for histological analysis.

Ink injections

To investigate the gross function of the cardiovascular system, the ventricle of E9.5 embryos was injected with Pelikan India ink diluted 50% in PBS (Luo et al., 2001). Before and after injection, embryos were kept at 37°C in a CO_2 incubator to maintain the heartbeat. After 4–6 h, embryos were examined under a dissecting microscope to see if the heart was beating, and then fixed and processed for photography.

Immunofluorescence staining

Embryos for α-actinin/Tmod1 staining in Fig. 6 were fixed overnight in freshly prepared 4% paraformaldehyde in PBS, followed by quenching in 50 mM NH_4Cl. Larger embryos (E9.5–12.5) were embedded in Tissue-Tek, and 8–12-μm sections were cut on a cryostat, while smaller embryos (E8–8.5 and E9.5 null) were labeled as whole mounts. To detect gaps in F-actin staining in the middle of sarcomeres, and to improve signal-to-noise by reducing cytoplasmic Tmod1 staining (Figs. 7–9), embryos were dissected in a relaxing buffer (Granzier et al., 1996) containing 1% Triton X-100, and incubated for 30 min on ice followed by fixation overnight in 4% paraformaldehyde in the same buffer. Embryos or sections were blocked in 4% BSA in PBS and labeled with primary antibodies overnight at 4°C, followed by fluorescent-conjugated secondary antibodies or bodipy-phallacidin (Gregorio and Fowler, 1995; Rudy et al., 2001). Primary antibodies were affinity-purified rabbit anti–human Tmod1 (R1749) (Fowler et al., 1993), mouse monoclonal anti–sarcomeric α-actinin (EA59) (Sigma-Aldrich), and mouse monoclonal anti-myomesin (B4; a gift from E. Ehler and J.-C. Perriard, Eidgenössische Technische Hochschule Zürich, Zurich, Switzerland) (Auerbach et al., 1997). Stained tissue was analyzed on a Bio-Rad Laboratories MRC1024 confocal scanning laser microscope with a Carl Zeiss MicroImaging, Inc. 63X lens (1.4 NA). Z stacks (0.54 μm per optical section) were collected for whole mount embryos and assembled and analyzed in Metamorph (Universal Imaging Corp.). Single image planes were used for figures, and contrast was adjusted using Adobe Photoshop 6.0®.

We thank Ryan Mudry and Andrea Grantham for histology and Todd Camensich for help in analyzing heart development in the mutant embryos.

Support for this research was provided by National Institutes of Health grants GM34225 to V.M. Fowler and HL57461 and HL03985 to C.C. Gregorio, and a grant from the Howard Hughes Institute for Medical Research to H.Y. Zoghbi. This is The Scripps Research Institute manuscript no. 15502-CB.

Submitted: 29 August 2003
Accepted: 17 October 2003

References

Almenar-Queralt, A., C.C. Gregorio, and V.M. Fowler. 1999a. Tropomodulin assembles early in myofibrillogenesis in chick skeletal muscle: evidence that thin filaments rearrange to form striated myofibrils. *J. Cell Sci.* 112:1111–1123.

Almenar-Queralt, A., A. Lee, C.A. Conley, L. Ribas de Pouplana, and V.M. Fowler. 1999b. Identification of a novel tropomodulin isoform, skeletal tropomodulin, that caps actin filament pointed ends in fast skeletal muscle. *J. Biol. Chem.* 274:28466–28475.

Auerbach, D., B. Rothen-Rutishauser, S. Bantle, M. Leu, E. Ehler, D. Helfman, and J.-C. Perriard. 1997. Molecular mechanisms of myofibril assembly in the heart. *Cell Struct. Funct.* 22:139–146.

Bamburg, J.R., A. McGough, and S. Ono. 1999. Putting a new twist on actin: ADF/cofilins modulate actin dynamics. *Trends Cell Biol.* 9:364–370.

Ben-Arie, H.N., H.J. Bellen, D.L. Armstrong, A.E. McCall, P.R. Gordadze, Q. Guo, M.M. Matzuk, and H.Y. Zoghbi. 1997. Math1 is essential for genesis of cerebellar granule neurons. *Nature.* 390:169–172.

Blanchard, E.M., K. Iizuka, M. Christe, D.A. Conner, A. Geisterfer-Lowrance, F.J. Schoen, D.W. Maughan, C.E. Seidman, and J.G. Seidman. 1997. Targeted ablation of the murine α-tropomyosin gene. *Circ. Res.* 81:1005–1010.

Bonnerot, C., and F.J. Nicolas. 1993. Clonal analysis in the intact mouse embryo by intragenic homologous recombination. *C. R. Acad. Sci. III.* 316:1207–1217.

Chu, X., D. Thompson, L.J. Yee, and L.A. Sung. 2000. Genomic organization of mouse and human erythrocyte tropomodulin genes encoding the pointed end capping protein for the actin filaments. *Gene.* 256:271–281.

Chu, X., J. Chen, M.C. Reedy, C. Vera, K.-L.P. Sung, and L.A. Sung. 2003. E-Tmod capping of actin filaments at the slow growing end is required to establish mouse embryonic circulation. *Am. J. Physiol. Heart Circ. Physiol.* 284: H1827–H1838.

Clark, K.A., A.S. McElhinney, M.C. Beckerle, and C.C. Gregorio. 2002. Striated muscle cytoarchitecture: An intricate web of form and function. *Annu. Rev. Cell Dev. Biol.* 18:637–706.

Du, A., J.M. Sanger, K.K. Linask, and J.W. Sanger. 2003. Myofibrillogenesis in the first cardiomyocytes formed from isolated quail precardiac mesoderm. *Dev. Biol.* 257:382–394.

Ehler, E., B.M. Rothen, S.P. Hammerle, M. Komiyama, and J.-C. Perriard. 1999. Myofibrillogenesis in the developing chicken heart: assembly of Z-disk, M-line and the thick filaments. *J. Cell Sci.* 112:1529–1539.

Ehler, E., R. Horowitz, C. Zuppinger, R.L. Price, E. Perriard, M. Leu, P. Caroni, M. Sussman, H.M. Eppenberger, and J.-C. Perriard. 2001. Alterations at the intercalated disk associated with absence of muscle LIM protein. *J. Cell Biol.* 153:763–772.

Fischer, R.S., and V.M. Fowler. 2003. Tropomodulins: life at the slow end. *Trends Cell Biol.* 13:593–601.

Epstein, H.F., and D.A. Fischman. 1991. Molecular analysis of protein assembly in muscle development. *Science.* 251:1039–1044.

Fowler, V.M. 1996. Regulation of actin filament length in erythrocytes and striated muscle. *Curr. Opin. Cell Biol.* 8:86–96.

Fowler, V.M., M.A. Sussman, P.G. Miller, B.E. Flucher, and M.P. Daniels. 1993. Tropomodulin is associated with the free (pointed) ends of the thin filaments in rat skeletal muscle. *J. Cell Biol.* 120:411–420.

Friedrich, G., and P. Soriano. 1991. Promoter traps in embryonic stem cells: a genetic screen to identify and mutate developmental genes in mice. *Genes Dev.* 5:1513–1523.

Granzier, H., M. Helmes, and K. Trombitas. 1996. Nonuniform elasticity of titin in cardiac myocytes: a study using immunoelectron microscopy and cellular mechanics. *Biophys. J.* 70:430–442.

Gregorio, C.C., and P.B. Antin. 2000. To the heart of myofibril assembly. *Trends Cell Biol.* 10:355–362.

Gregorio, C.C., and V.M. Fowler. 1995. Mechanisms of myofibril assembly in embryonic chick cardiac myocytes. *J. Cell Biol.* 129:683–695.

Gregorio, C.C., A. Weber, M. Bondad, C.R. Pennise, and V.M. Fowler. 1995. Requirement of pointed end capping by tropomodulin to maintain actin fila-

ment length in embryonic chick cardiac myocytes. *Nature.* 377:83–86.

Holtzer, H., T. Hijikata, Z.X. Lin, Z.Q. Zhang, S. Holtzer, F. Protasi, C. Franzini-Armstrong, and H.L. Sweeney. 1997. Independent assembly of 1.6 microns long bipolar MHC filaments and I-Z-I bodies. *Cell Struct. Funct.* 22:83–93.

Ito, M., B. Swanson, M.A. Sussman, L. Kedes, and G. Lyons. 1995. Cloning of tropomodulin cDNA and localization of gene transcripts during mouse embryogenesis. *Dev. Biol.* 167:317–328.

Kazmierski, S.T., P.B. Antin, C.C. Witt, N. Huebner, A.S. McElhinny, S. Labeit, and C.C. Gregorio. 2003. The complete mouse nebulin gene sequence and the identification of cardiac nebulin. *J. Mol. Biol*. 328:835–846.

Littlefield, R., and V.M. Fowler. 1998. Defining actin filament length in striated muscle: rulers and caps or dynamic stability? *Annu. Rev. Cell Dev. Biol.* 14: 487–525.

Littlefield, R., and V.M. Fowler. 2002. Measurements of thin filament lengths by distributed deconvolution analysis of fluorescence images. *Biophys. J.* 82: 2548–2564.

Littlefield, R., A. Almenar-Queralt, and V.M. Fowler. 2001. Actin dynamics at pointed ends regulates thin filament length in striated muscle. *Nat. Cell Biol.* 3:544–551.

Luo, Y., M.C. Ferreira-Cornwell, M.S. Baldwin, I. Kostetskii, J.M. Lenox, M. Lieberman, and G.L. Radice. 2001. Rescuing the N-cadherin knockout by cardiac-specific expression of N- or E-cadherin. *Development.* 128:459–469.

Markwald, R. 1973. Distribution and relationship of precursor Z material to organizing myofibrillar bundles in embryonic rat and hamster ventricular myocytes. *J. Mol. Cell. Cardiol.* 5:341–350.

McElhinney, A.S., B. Kolmerer, V.M. Fowler, S. Labeit, and C.C. Gregorio. 2001. The N-terminal end of nebulin interacts with tropomodulin at the pointed ends of the thin filaments. *J. Biol. Chem.* 276:583–592.

Mudry, R.E., C.N. Perry, M. Richards, V.M. Fowler, and C.C. Gregorio. 2003. The interaction of tropomodulin with tropomyosin stabilizes thin filaments in cardiac myocytes. *J. Cell Biol*. 162:1057–1068.

Nyakern-Meazza, M., K. Narayan, C.E. Schutt, and U. Lindbergh. 2002. Tropomyosin and gelsolin cooperate in controlling the microfilament system. *J. Biol. Chem.* 277:28774–28779.

Ono, S., and K. Ono. 2002. Tropomyosin inhibits ADF/cofilin-dependent actin filament dynamics. *J. Cell Biol.* 156:1065–1076.

Ono, S., D.L. Baillie, and G.M. Benian. 1999. UNC-60B, an ADF/cofilin family protein, is required for proper assembly of actin into myofibrils in *Caenorhabditis elegans* body wall muscle. *J. Cell Biol.* 145:491–502.

Radice, G.L., H. Rayburn, H. Matsunami, K.A. Knudsen, M. Takeichi, and R.O. Hynes. 1997. Developmental defects in mouse embryos lacking N-cadherin. *Dev. Biol.* 181:64–78.

Rethinasamy, P., M. Muthuchamy, T. Hewett, G. Boivin, B.M. Wolska, C. Evans, R.J. Solaro, and D.F. Wieczorek. 1998. Molecular and physiological effects of α-tropomyosin ablation in the mouse. *Circ. Res.* 82:116–123.

Rudy, D.E., T.A. Yatskievych, P.B. Antin, and C.C. Gregorio. 2001. Assembly of thick, thin, and titin filaments in chick precardiac explants. *Dev. Dyn.* 221: 61–71.

Sehnert, A.J., and D.Y.R. Stainier. 2002. A window to the heart: can zebrafish mutants help us understand heart disease in humans? *Trends Genet.* 18:491–494.

Seidman, J.G., and C. Seidman. 2001. The genetic basis for cardiomyopathy: from mutation identification to mechanistic paradigms. *Cell.* 104:557–567.

Sussman, M.A., S. Baque, C.-S. Uhm, M.P. Daniels, R.L. Price, D. Simpson, L. Terracio, and L. Kedes. 1998a. Altered expression of tropomodulin in cardiomyocytes disrupts the sarcomeric structure of myofibrils. *Circ. Res.* 82:94–105.

Sussman, M.A., S. Welch, N. Cambon, R. Klevitsky, T.E. Hewett, R. Price, S.A. Witt, and T.R. Kimball. 1998b. Myofibril degeneration caused by tropomodulin overexpression leads to dilated cardiomyopathy in juvenile mice. *J. Clin. Invest.* 101:51–61.

Tokuyasu, K.R., and P.A. Maher. 1987. Immunocytochemical studies of cardiac myofibrillogenesis in early chick embryos. I. Presence of immunofluorescent titin spots in premyofibril stages. *J. Cell Biol.* 105:2781–2793.

Vigoreaux, J.O. 2001. Genetics of the *Drosophila* flight muscle myofibril: a window into the biology of complex systems. *Bioessays.* 23:1047–1063.

Watakabe, A., R. Kobayashi, and D.M. Helfman. 1996. N-tropomodulin: a novel isoform of tropomodulin identified as the major binding protein to brain tropomyosin. *J. Cell Sci.* 109:2299–2310.

Weber, A., C.R. Pennise, G.G. Babcock, and V.M. Fowler. 1994. Tropomodulin caps the pointed ends of actin filaments. *J. Cell Biol.* 127:1627–1635.

Weber, A., C.R. Pennise, and V.M. Fowler. 1999. Tropomodulin increases the critical concentration of barbed end-capped actin filaments by converting ADP-Pi actin to ADP-actin at all pointed ends. *J. Biol. Chem.* 274:34637–34645.